ORIGINAL RESEARCH

American Heart Association | American Stroke Association

Rad GTPase Deletion Increases L-type Calcium Channel Current Leading to Increased Cardiac Contraction

Janet R. Manning, PhD; Guo Yin, MS; Catherine N. Kaminski, BS; Janos Magyar, PhD; Han-Zhong Feng, PhD; John Penn, MS; Gail Sievert, MS; Katherine Thompson, PhD; J.-P. Jin, PhD; Douglas A. Andres, PhD; Jonathan Satin, PhD

***Background*—**The small GTPase Rad is a negative regulator of voltage-dependent L-type calcium channel current (I_{CaL}); however, the effects of Rad ablation on cardiomyocyte function are unknown. The objective of this study is to test the hypothesis that Rad-depletion causes positive inotropic effects without inducing cardiac hypertrophy.

***Methods and Results*—**Ventricular myocytes from adult $Rad^{-/-}$ mice were isolated and evaluated by patch-clamp recordings for $I_{Ca,L}$ and action potentials, Ca^{2+} transients, and sarcomere shortening. Maximum I_{CaL} is elevated in $Rad^{-/-}$ (maximal conductance 0.35±0.04 picoSiemens/picoFarad (pS/pF) wild-type; 0.61±0.14 pS/pF $Rad^{-/-}$), decay kinetics are faster, and $I_{Ca,L}$ activates at lower voltages (activation midpoint −7.2±0.6 wild-type; −11.7±0.9 $Rad^{-/-}$) mimicking effects of β-adrenergic receptor stimulation. Diastolic and twitch calcium are elevated in $Rad^{-/-}$ ($F_{340/380}$: 1.03 diastolic and 0.35 twitch for wild-type; 1.47 diastolic and 0.736 twitch for $Rad^{-/-}$) and sarcomere shortening is enhanced (4.31% wild-type; 14.13% $Rad^{-/-}$) at lower pacing frequencies. Consequentially, frequency-dependence of Ca^{2+} transients is less in $Rad^{-/-}$, and the frequency dependence of relaxation is also blunted. In isolated working hearts, similar results were obtained; chiefly, +dP/dt was elevated at baseline and developed pressure was relatively nonresponsive to acute β-adrenergic receptor stimulation. In single cells, at subphysiological frequencies, nonstimulated calmodulin-dependent protein kinase–sensitive calcium release is observed. Remarkably, $Rad^{-/-}$ hearts did not show hypertrophic growth despite elevated levels of diastolic calcium.

***Conclusions*—**This study demonstrates that the depletion of Rad GTPase is equivalent to sympathomimetic β-adrenergic receptor, without stimulating cardiac hypertrophy. Thus, targeting Rad GTPase is a novel potential therapeutic target for Ca^{2+}-homeostasis–driven positive inotropic support of the heart. **(*J Am Heart Assoc*. 2013;2:e000459 doi: 10.1161/JAHA.113.000459)**

Key Words: inotropy • L-type calcium current • Rad • RGK • β-adrenergic stimulation

The cardiac inotropic response is regulated by excitation-contraction coupling. Voltage-gated L-type calcium-channel (LTCC) opening is stimulated by depolarization, and the degree and duration of LTCC-mediated Ca^{2+} influx are modulated by a number of factors, including Ca^{2+}, calmodulin (CaM), and interactions with a variety of auxiliary proteins. LTCC current is at the top of a cascade of events that initiate excitation-contraction coupling and thus regulates the strength of cardiac contraction. LTCC blockers can cause a negative inotropism; conversely, any agent that increases LTCC Ca^{2+} current ($I_{Ca,L}$) might, in theory, serve as a positive inotrope. In current practice, however, no such regimens are used. Pharmacologically, inotropic support is targeted via Ca^{2+} sensitizers or via manipulation of Ca^{2+} homeostasis secondary to partial interference with the sodium-potassium ATPase function.[1]

The major physiological mechanism for modulating cardiac output is sympathetic stimulation. This is mediated in large part by agonist stimulation of β-adrenergic receptors (β-ARs) coupled to LTCC. The pore-forming subunit of the LTCC, $Ca_V1.2$, and auxiliary proteins such as $Ca_V\beta2$ contain substrates for β-AR–mediated phosphorylation. Although the molecular mechanism remains incompletely understood, β-AR modulation of LTCC results in shifts of LTCC voltage activation and increases in maximal macroscopic conductance. Increased $I_{Ca,L}$ triggers additional sarcoplasmic reticulum (SR) Ca^{2+} release. In turn, increased Ca^{2+} release promotes negative feedback via increased Ca^{2+}-CaM–dependent inactivation.[2]

From the Departments of Physiology (J.R.M., G.Y., J.M., J.P., G.S., J.S.), Molecular and Cellular Biochemistry (J.R.M., C.N.K., D.A.A.), and Statistics (K.T.), University of Kentucky College of Medicine, Lexington, KY; Department of Physiology, University of Debrecen, Hungary (J.M.); Department of Physiology, Wayne State University School of Medicine, Detroit, MI (H.-Z.F., J.-P.J.).

Correspondence to: Jonathan Satin, PhD, Department of Physiology, MS-508, University of Kentucky College of Medicine, 800 Rose St, Lexington, KY 40536-0298. E-mail: jsatin1@uky.edu

Received September 5, 2013; accepted November 11, 2013.

There is reward and risk in modulating Ca^{2+} homeostasis via up-regulation of LTCC function. In the normal sequence of events, contractile Ca^{2+} is supplied by LTCC triggering of ryanodine receptor (RyR_2)-mediated influx from the SR, making LTCC a potential point of contractile function regulation. However, inappropriate SR Ca^{2+} release is likely causative in a variety of cardiac arrhythmias.[3] Augmentation of $I_{Ca,L}$ has been proposed as a major contributing factor to arrhythmogenesis,[4,5] and blocking $I_{Ca,L}$ suppresses ventricular arrhythmogenesis.[6] Thus, $I_{Ca,L}$ is a focal point in the regulation of cardiac action potential (AP), excitation-contraction coupling, and arrhythmogenesis.[7] Nonetheless, there are few model systems with chronic elevation selectively of LTCC activity to test this hypothesis.

The cardiac LTCC is a heteromultimeric complex. Accessory proteins include, but are not limited to, $Ca_V\beta2$, $Ca_V\alpha2\delta$, CaM, and CaM-dependent protein kinase (CaMKII). Each of these auxiliary proteins co-localizes with $Ca_V1.2$, forming a native LTCC complex. More recently discovered members of this complex include the RGK (Rad, Gem/Kir) family, which consists of small GTPases that can bind to and regulate LTCC.[8] Overexpression of all known RGK proteins leads to a profound blockade of $I_{Ca,L}$.[9–11] Conversely, deletion of selected RGK proteins does not necessarily lead to a dramatic up-regulation of $I_{Ca,L}$ in cardiomyocytes.[12] Loss of function of Rad, via either RNAi-mediated knockdown or overexpression of a dominant negative mutant increases $I_{Ca,L}$, Ca^{2+} transients, and contractility.[13] Enhanced LTCC function can induce activation of CaMKII, which in turn prolongs QT interval and creates a substrate for bradycardia-induced arrhythmias.[3] $Rad^{-/-}$ mice display elevated phosphorylated-CaMKII[14] and increased heart growth in response to pressure overload,[14] but there are no reports of the effect of deletion of Rad on myocardial function. Cardiac arrhythmias are comorbid with cardiac hypertrophy.[15] Therefore, in this study we tested the hypothesis that Rad is a key contributor to cardiac electrical function. We studied $I_{Ca,L}$, Ca^{2+} handling, APs, contractile function at the cellular and heart organ level, and heart electrical activity from $Rad^{-/-}$ mice. Here, we report that the absence of Rad expression mimics tonic β-adrenergic stimulation of electrical and contractile properties without gross cardiac hypertrophy and without arrhythmia at physiologically relevant frequencies.

Materials and Methods

All experimental procedures and protocols were approved by the Animal Care and Use Committee of the University of Kentucky and Wayne State University and conformed to the National Institutes of Health "Guide for the Care and Use of Laboratory Animals."

Ventricular Myocyte Isolation

Isolated ventricular cardiomyocytes were prepared as previously described[12] (see Detailed Methods for further details).

Single-Cell Assays: Electrophysiological Recordings and Calcium Transients

$I_{Ca,L}$ was recorded in the whole-cell configuration of the patch-clamp technique as previously described.[12] All recordings were performed at room temperature (20° to 22°C). The pipette solution consisted of (in mmol/L) 125 Cs-methanesulfonate, 15 TEA-Cl, 1 $MgCl_2$, 10 EGTA, and 5 HEPES, pH 7.2. Bath solution contained (in mmol/L) 150 NMDG, 2.5 $CaCl_2$, 1 $MgCl_2$, 10 glucose, 10 HEPES, and 5,4-aminopyridine, pH 7.2. AP recordings were performed in a physiological saline solution consisting of (in mmol/L) 140 NaCl, 1.8 $CaCl_2$, 1 $MgCl_2$, 5.4 KCl, 10 glucose, and 10 HEPES, pH 7.25. For AP recordings, the pipette solution contained (in mmol/L) 115 K-glutamate, 45 KCl, 3.0 Mg-ATP, and 10.0 HEPES, pH 7.21 (KOH). All AP recordings were performed at room temperature (20° to 22°C). Activation voltage dependence parameters were obtained by fitting the current-voltage slope conductance transform to a Boltzmann distribution of the form $G(V)=G_{max}/[1+\exp(V_{½}/k)]$, where G_{max} is the maximal conductance and $V_{½}$ is the activation midpoint.

Ca^{2+} transients were recorded from ventricular cardiomyocytes loaded with cell permeable Fura-2-AM (Invitrogen). Additional details are available in Detailed Methods.

Ex Vivo Working Heart Studies

Hearts were excised from age-matched adult wild-type and $Rad^{-/-}$ mice and perfused on a Langendorff-Neely isolated working heart preparation as previously described.[16] Functional parameters were tested at 10 mm Hg of preload and 55 mm Hg of afterload before and after 10 nmol/L isoproterenol treatment.

ECG Telemetry

Mice were implanted with Data ART TA-F10 transmitters and allowed to recover for 14 days prior to initiation of recordings.

Statistical Analysis

For statistical analyses performed on all cellular observations, the mouse is the primary unit of analysis. Intercellular variations within each isolation (mouse) were accounted for by using a nested algorithm. For simplicity, cellular mean and SEM values are represented in the figures. The within-mouse

averages of the cellular observations were used for analysis to perform the analysis on the level of the experimental units, the mice. To normalize the data, the log transform of the following variables was taken prior to analysis: diastolic calcium and level twitch calcium level. The factors of mouse type, KN93, isoproterenol treatment were analyzed using factorial ANOVA. In the studies of responses across multiple frequencies, a repeated-measures ANOVA was performed using cells for which data were obtained at all frequencies. Data that are not missing at random are excluded from the frequency plot; however, data on all cells were included at the frequency of 1 Hz for the statistical analyses. Post-hoc t tests were performed to compare particular groups of interest. In the analyses involving difference of means between wild-type and $Rad^{-/-}$ mice under the assumption of normality of the response variable, including isolated heart functional data (Figure 10) and heart rate data (Figure 12), 2-sample t tests were used, and paired t tests were used for before and after isoproterenol treatment comparisons. All ANOVAs were performed using PROC GLM (SAS Institute Inc).

Detailed Methods

Animals and Surgery

Mice lacking Rad expression ($Rad^{-/-}$) were generated and characterized as previously described[14] with no overt gross cardiac phenotype.

The Rad knockout and littermate control mice used in this study were obtained from the Kahn laboratory at the Joslin Diabetes Center. As described previously, mice were derived from a 129/SvJ1 embryonic stem cell clone injected into C57BL/6 blastocytes to produce chimeras, which were subsequently crossed with C57BL/6 mice for 5 generations.[14] Mice used in this study were the offspring of these founders.

Rad knockout mice and wild-type cohorts were implanted with subcutaneous radiotelemeters (Data Sciences International). Preoperative evaluation included daily observation to ensure the mice were active and had a clean smooth coat, clear eyes and nares, and no evidence of diarrhea or respiratory distress. Preoperative anesthesia consisted of 2% to 3% isoflurane in 100% oxygen at 1 L/min. Anesthetic depth was measured as loss of withdrawal and corneal reflexes. Postoperative analgesia was provided (carprofen 10 mg/kg via subcutaneous injection and then every 12 hours for 48 hours). ECG recordings were taken after a 2-week postsurgical recovery period. After establishing a 24-hour baseline, mice were injected intraperitoneally with carbachol (0.5 mg/kg), and ECGs were monitored to confirm bradycardia. Waveform parameters, including QT intervals were recorded and analyzed using DataquestART 4.0 software (Data Sciences International).

Ventricular Myocyte Isolation

Adult ventricular myocyte isolation was performed as in previous studies.[12] Prior to heart excision mice were anesthetized with ketamine+xylazine (90+10 mg/kg intraperitoneally). Hearts were excised from adult $Rad^{-/-}$ and wild-type and immediately perfused on a Langendorff apparatus with a high-potassium Tyrode buffer and then digested with 5 to 7 mg liberase (Roche). After digestion, atria were removed and ventricular myocytes were mechanically dispersed. Calcium concentrations were gradually restored to physiological levels in a stepwise fashion, and only healthy quiescent ventricular myocytes were used for electrophysiological analysis or calcium imaging within 12 hours.

I_{CaL} and AP Measurements

Inward current from adult ventricular $Rad^{-/-}$ or wild-type myocytes was measured in the presence of inhibited sodium and potassium channels, to isolate inward current from calcium, with internal calcium weakly buffered with EGTA. Additionally, APs were obtained at various frequencies after establishing steady state. For AP recordings, internal and external solutions contain physiological concentrations of sodium, potassium, and calcium. Specific ionic conditions were given in Materials and Methods.

Cytosolic Calcium Measurements

Adult ventricular myoctyes loaded with cell-permeable Fura-2 AM were paced at 1.0 Hz to determine fractional shortening and sarcomere length. All measurements were made following >5 minutes of conditioning 1-Hz field stimuli to induce steady state. Transients were recorded at 0.5, 1.0, 2, and 3 Hz, after which pacing frequency was reduced to 0.1 Hz and extraneous transients were counted. To determine SR load, cells were paced at 1.0 Hz until transients reached steady state, and then pacing was stopped and bath calcium was reduced to 0 contemporaneously. After 20 s in 0 calcium bath, a pulse of caffeine (50 mmol/L) was administered locally to the cell and the resulting peak calcium transient was measured (Figure 9). To determine the role of CaMKII in $Rad^{-/-}$ calcium homeostasis, a separate cohort of cells were preincubated in 1 μmol/L KN93 for 30 minutes and then subjected to the same protocol. All data were analyzed using IonOptix IonWizard 6.3. Background fluorescence (Fbackground) for F380 and F340 were determined from cell-free regions. Fo was determined from the steady-state ratio following caffeine release in calcium- and sodium-free bath solution. Data are expressed as F340/380 and were corrected for Fbackground.

Immunoblotting

Hearts freshly excised from wild-type and $Rad^{-/-}$ mice (Figure 11C) or perfused on a Langendorff apparatus (Figure 6D) were flash frozen, and tissue was pulverized under liquid nitrogen before homogenization in cell lysis buffer containing 20 mmol/L HEPES, pH 7.4, 50 mmol/L KF, 50 mmol/L β-glycerol phosphate, 150 mmol/L NaCl, 2 mmol/L EGTA, pH 8.0, 0.5% Triton X-100, 10% glycerol, 2 mmol/L $Na3VO_4$, and 1× protease inhibitor cocktail (Calbiochem). Lysates were centrifuged at 13 000 rpm, and the protein concentrations of the supernatants were measured. Lysates were prepared in 4× SDS-PAGE loading buffer, and 30 μg total protein per lane was resolved on 15% SDS-PAGE gels and transferred to nitrocellulose membranes. Phospholamban phosphorylation levels were measured by immunoblotting with phospholamban phosphoserine 16 (1:5000, Badrilla), phospho-threonine 17 (1:5000, Badrilla), and total (1:500, Thermo Scientific) antibodies. Proteins were detected using SuperSignal enhanced chemiluminescence (Pierce), and immunoblots were developed and quantified using the BioRad ChemiDoc MP Imaging System.

Ex Vivo Working Heart Studies

Hearts were excised from adult $Rad^{-/-}$ and wild-type mice and perfused in a Langendorff-Neely isolated working heart preparation as previously described.[16] Briefly, the aorta was quickly cannulated and the heart was subjected to retrograde perfusion of oxygenated Krebs-Henseleit buffer containing (in mmol/L) NaCl 118, mmol/L KCl 4.7, $CaCl_2$ 2.25, $MgSO_4$ 2.25, KH_2PO 1.2, EGTA 0.32, $NaHCO_3$ 25, and D-glucose 11) <60 s after removal. The left atrium was subsequently cannulated, and the heart was switched to anterograde perfusion with a constant preload of 10 mm Hg and constant afterload of 55 mm Hg. The working heart supraventricularly paced throughout the study at a rate slightly higher than the intrinsic rate. Left ventricular pressure, cardiac output, and coronary flow were measured once the heart had reached steady state. To examine the effects of β-adrenergic stimulation, isoproterenol (10 nmol/L) was added to the perfusate, and after reaching steady-state, the same functional parameters were measured.

Results

Rad Deletion Increases $I_{Ca,L}$ and Predicted Window $I_{Ca,L}$

Rad overexpression profoundly inhibits $I_{Ca,L}$ in heterologous expression systems.[9] However, our recent findings in $Rem^{-/-}$ cardiomyocytes show that LTCC voltage dependence is shifted positive, suggesting that physiological expression levels of RGK proteins may act to fine-tune $I_{Ca,L}$.[12,17] To examine the contribution of Rad to LTCC function, we measured $I_{Ca,L}$ in mature $Rad^{-/-}$ cardiomyocytes. Figure 1A shows representative $I_{Ca,L}$ traces. There is a robust persistent inward $I_{Ca,L}$ for relatively low V_{test} (Figure 1A, note V_{test} −35 mV). $I_{Ca,L}$ traces for steady-state activation and availability were obtained. Peak current density at membrane potentials corresponding to maximal conductance (V_{test} +20 mV) was increased in $Rad^{-/-}$ (−10.1±1.7 pA/pF; G_{max} 0.61±0.14 pS/pF; n=12) compared with wild-type (−6.6±0.8 pA/pF; G_{max} 0.35±0.04 pS/pF; n=11; Figure 1B). The kinetics of $I_{Ca,L}$ decay were not significantly different for V_{test} positive to −10 mV; however, for the low-voltage range of V_{test}, there was a relatively fast decay component in $Rad^{-/-}$ cardiomyocytes (Figure 1C). The voltage dependence of $I_{Ca,L}$ activation and availability is well described with Boltzmann distributions. There is no significant difference in steady-state availability between wild-type and $Rad^{-/-}$. By contrast, the voltage dependence of $Rad^{-/-}$ steady-state activation is significantly shifted ≈−5 mV compared with wild-type (Figure 1D, V½=−7.2±0.6 [n=11 cells] and −11.7±0.9 [n=12 cells], for wild-type and $Rad^{-/-}$, respectively). Consequently, the window current formed by the intersection of availability and activation is increased in $Rad^{-/-}$ cardiomyocytes.

APs integrate the combined function of the sum of ion channels, pumps, and exchangers. $Rad^{-/-}$ $I_{Ca,L}$ is larger but decays faster, thus complicating an a priori prediction of resulting AP properties. Mouse APs are relatively fast compared with nonrodent mammals. Wild-type cardiomyocyte APs show typical rapid repolarization, along with a slower phase of repolarization negative to −45 mV (Figure 2A). In contrast, $Rad^{-/-}$ ventricular cardiomyocyte AP morphology contains a more prominent inflection point positive to 0 mV and a more pronounced plateau phase (Figure 2B, arrows). Wild-type AP duration (APD) increased for stimulation frequencies slower than 1 Hz, and APD showed imperceptible differences between 1 and 3 Hz (Figure 3). $Rad^{-/-}$ APD was not significantly different from wild-type between 1 and 3 Hz (Figure 3). APD is largely influenced by the action of LTCC, by the balance of other ion channel conductances, and by Ca^{2+} handling. We surmised that $Rad^{-/-}$ LTCC complexes would allow excessive Ca^{2+} entry and that this would be exacerbated at lower stimulation frequencies secondary to accumulation of slow recovery from inactivation at very low pacing frequencies. To test this, we measured APs and Ca^{2+} transients at 0.1 Hz (Figure 2C). During the relatively long quiescent intervals, we observed a progressive depolarization of most $Rad^{-/-}$ cardiomyocytes (not shown). In slowly paced $Rad^{-/-}$ cells, maintaining diastolic membrane potential negative to −70 mV was not possible. Figure 2C shows a representative afterdepolarization from $Rad^{-/-}$ cardiomyocytes (observed in 9 of 11 cells tested). Changing stimulation frequency back to 1 Hz converted the AP

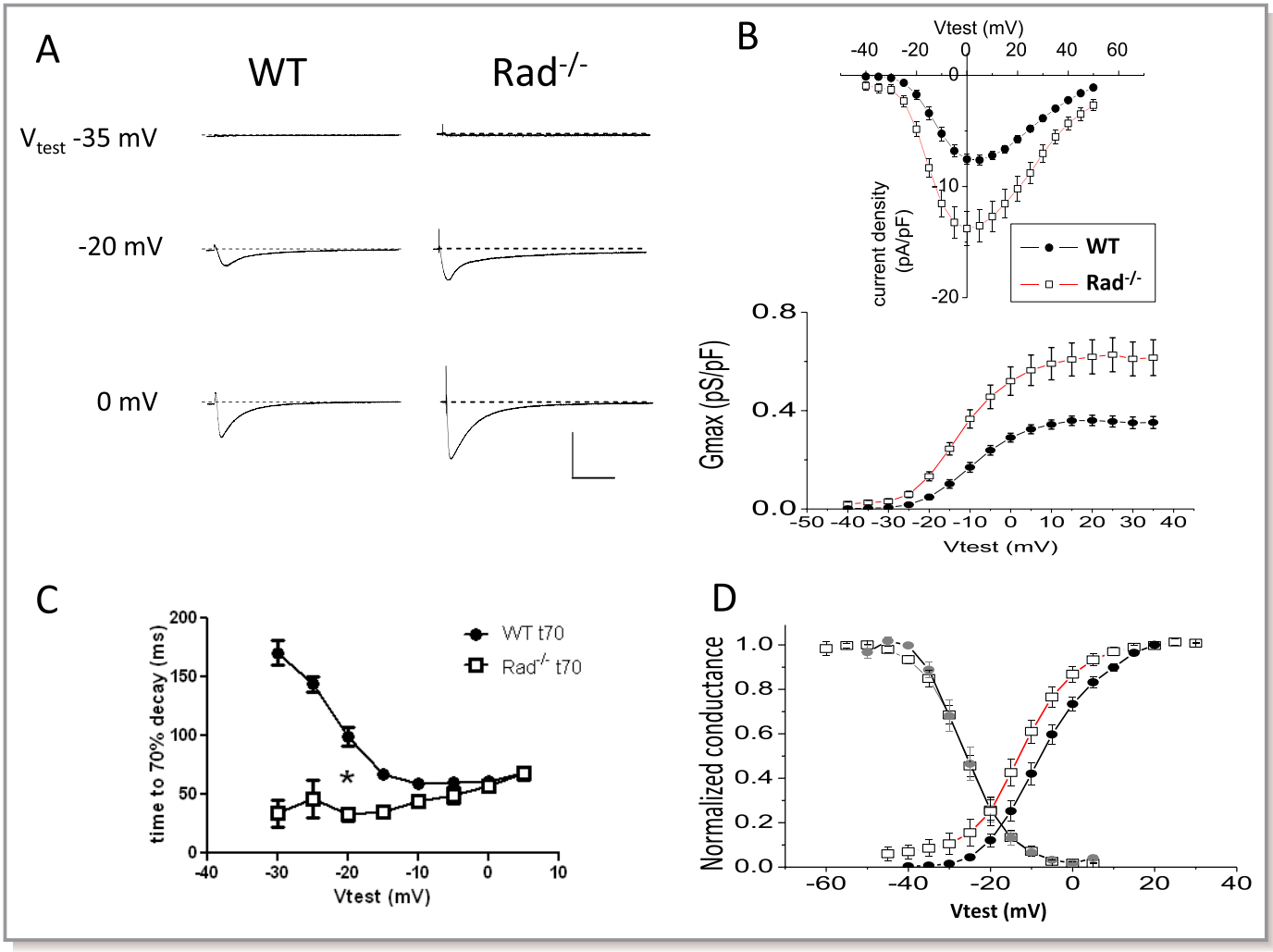

Figure 1. Rad$^{-/-}$ $I_{Ca,L}$ activation is negative-shifted revealing increased predicted $I_{Ca,L}$ window. A, Representative $I_{Ca,L}$ traces for V_{test} −35, −20, and 0 mV. Note greater current from Rad$^{-/-}$ cardiomyocyte for V_{test} −35 mV. Scale bars: 5 pA/pF and 100 ms. B, Current density is significantly increased in Rad$^{-/-}$ vs wild-type (WT). Below the current–voltage curve is a conductance–voltage curve illustrating the increased maximal conductance normalized to membrane capacitance. C, Calcium decay kinetics measured as time to 70% of baseline. D, Conductance–voltage curves for steady-state inactivation and activation in WT (squares) and Rad$^{-/-}$ (circles). Smooth lines are fitted Boltzmann distributions. n=11 cells and 12 cells for WT and Rad$^{-/-}$, respectively. Error bars represent SEM. $I_{Ca,L}$ indicates L-type calcium channel current.

morphology to that shown in Figure 2B. We did not observe afterdepolarizations in wild-type cells (0 of 12 cells). These findings are consistent with elevated Ca^{2+}-entry via $I_{Ca,L}$ window, but only for ultralow, nonphysiological frequencies. It follows that the increased stimulation frequency prevents afterdepolarization in Rad$^{-/-}$ via accumulated inactivated channels.

Rad$^{-/-}$ Cardiomyocytes Show Elevated Systolic and Diastolic Ca^{2+} and Spontaneous Ca^{2+} Transients Only at Extremely Low Frequencies

The increased calcium current observed on Rad ablation is expected to produce a parallel effect on cytosolic calcium levels. Cytosolic calcium transients were therefore measured in Rad$^{-/-}$ and wild-type isolated ventricular myocytes. Pacing frequencies ranged from 0.5 Hz to 3 Hz (Figures 4 and 5A, 5B). Diastolic cytosolic Ca^{2+} in wild-type cardiomyocytes progressively increases with increasing pacing frequency, as expected. By contrast, Rad$^{-/-}$ cardiomyocyte diastolic Ca^{2+} is elevated at relatively low frequencies (Figure 5C). Additionally, the peak amplitude of twitch calcium was found to be elevated in Rad$^{-/-}$ compared with wild-type (Figure 5D). Diastolic calcium in Rad$^{-/-}$ cardiomyocytes is not altered at higher stimulation frequencies (Figure 5E and 5F). SR Ca^{2+} content measured as caffeine-releasable Ca^{2+} is not significantly different between wild-type and Rad$^{-/-}$ (Figure 6). Transient decay kinetics (τ) were measured for pacing frequencies ranging from 0.1 Hz to 1 Hz to determine whether frequency-dependent acceleration of relaxation (FDAR) is altered by the loss of Rad. The relaxation

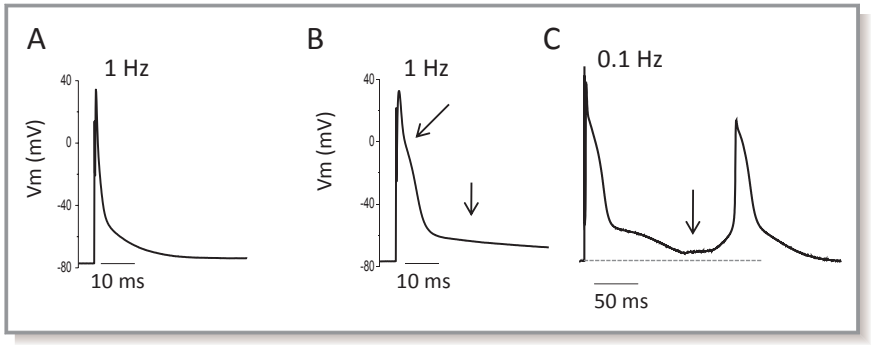

Figure 2. Rad$^{-/-}$ cardiomyocytes show very low frequency–dependent afterdepolarizations. A through C, Representative action potentials (APs) displaying (A) wild-type AP morphology and (B and C) Rad$^{-/-}$ AP morphology at (B) 1.0 Hz and (C) 0.1 Hz.

of Rad$^{-/-}$ is significantly faster at 0.1 Hz, although no significant difference was observed at 1 Hz (Figure 5G and 5H). We simultaneously measured sarcomere length. Elevated diastolic Ca^{2+} corresponds with a trend toward shorter resting sarcomere length (Figure 5I) and, as expected from increased twitch Ca^{2+} transient amplitude fractional shortening, is also significantly increased in Rad$^{-/-}$ at 1 Hz (14.13±1.67%; n=16 cells from 3 mice) compared with wild-type (4.31±0.742%, n=16 cells from 3 mice; Figure 5J), suggesting an increase in contractility in Rad$^{-/-}$ ventricular myocytes.

Ultralow-frequency stimulation of Rad$^{-/-}$ cardiomyocytes results in electrical afterdepolarizations presumably via cytosolic Ca^{2+} overload (Figure 2C). To further explore this notion, we paced cardiomyocytes at 3 Hz and changed stimulation frequency to 0.1 Hz. In wild-type cardiomyocytes, diastolic Ca^{2+} settles to a lower level, and there is rarely any activity between stimuli (Figure 7A). By contrast, Rad$^{-/-}$ cardiomyocytes show significantly increased spontaneous Ca^{2+} transients during interpulse intervals (Figure 7B and 7C). These results are consistent with the notion that excessive $I_{Ca,L}$ window and low-voltage activation can trigger spontaneous Ca^{2+} transients. It was noted previously that Rad$^{-/-}$ mouse hearts have elevated CaMKII activity compared with wild-type cardiomyocytes under conditions that promote hypertrophic heart growth.[14] Thus, it is plausible that tonic diastolic Ca^{2+} entry may drive CaMKII activity to promote spontaneous Ca^{2+} transients at subphysiological frequencies. To test this idea, we treated cardiomyocytes with KN93, a CaMKII inhibitor. Figure 8A shows representative Ca^{2+} transients illustrating that treating Rad$^{-/-}$ cells with KN93 results in diastolic Ca^{2+} indistinguishable from wild-type levels and restores the dynamic range of the Ca^{2+} transient response to that seen

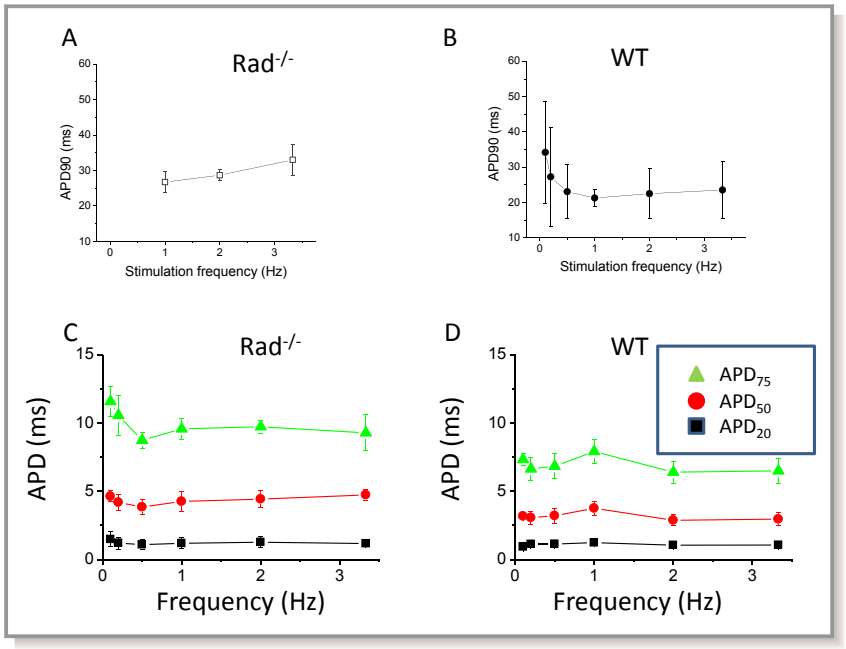

Figure 3. Action potential duration (APD). A, Frequency-dependent afterdepolarizations resulting spontaneous AP (arrow) are observed at 0.1 Hz. B, Frequency-dependent APD changes in wild-type (WT) (D) and Rad$^{-/-}$ (E) cells. n=12 WT cells (3 mice); n=12 cells (7 mice) per group. C and D, APD <90% are not significantly different between Rad$^{-/-}$ (left) and WT (right). APD_{20}, APD_{50}, and APD_{75} are shown for each. WT indicates wild-type.

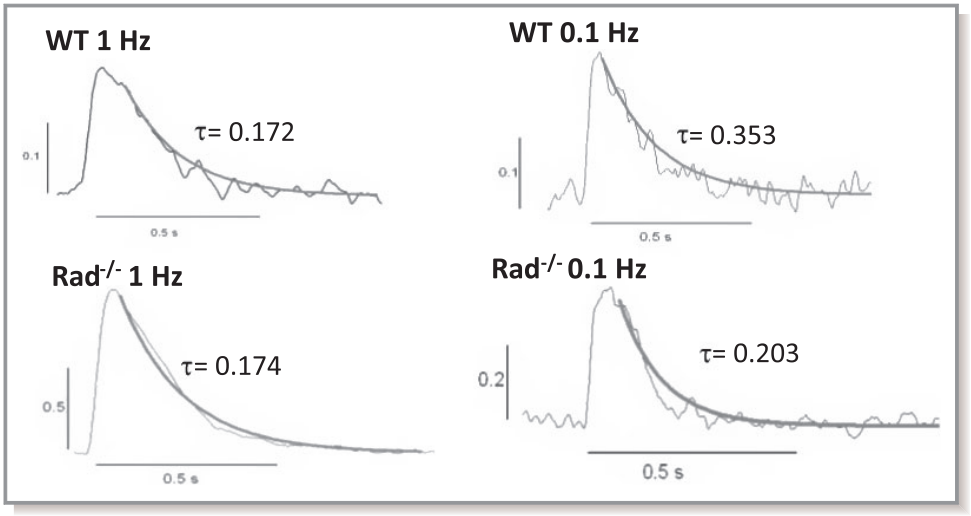

Figure 4. Expanded view of representative Ca^{2+} transients superimposed with single exponential fitted curve. WT indicates wild-type.

in wild-type, (Figure 8B and 8C). Moreover, KN93 also blocks spontaneous Ca^{2+} release. Figure 8D shows representative Ca^{2+} transients for cells paced at 3 Hz followed by 0.1 Hz showing spontaneous Ca^{2+} transients (as earlier). The addition of KN93 significantly reduces $Rad^{-/-}$ spontaneous Ca^{2+} transients to a level indistinguishable from wild-type (Figure 8D and 8E). KN92, in the inactive homolog of KN93, had no significant effect on unstimulated Ca^{2+} transients (Figure 8F). Furthermore, CaMKII phosphorylation status as an index of CaMKII activity was measured in untreated wild-type and $Rad^{-/-}$ hearts. $Rad^{-/-}$ hearts show increased phosphorylated CaMKII consistent with KN-93–sensitive spontaneous Ca^{2+} transients (Figure 8E and 8G).

Absence of Rad Causes LTCC Effects That Mimic Tonic β-Adrenergic Receptor Modulation, Including Loss of β-Adrenergic Agonism

The negative shift of the $V_{½}$ for activation of $Rad^{-/-}$ $I_{Ca,L}$ is suggestive of tonic β-AR modulation and would be consistent with the hypothesis that Rad contributes to a dampening of $I_{Ca,L}$ such as that for unstimulated conditions Rad prevents LTCC modulation. It then follows that the absence of Rad creates a permissive condition for β-AR–like modulation of LTCC despite the absence of agonist. To probe this provocative idea, we tested the effect of acute isoproterenol stimulation on $I_{Ca,L}$, Ca^{2+} transients, sarcomere shortening, and heart contraction. We predicted that basal properties in $Rad^{-/-}$ would be unchanged by acute isoproterenol treatment. The steady-state activation midpoint is significantly negative shifted in wild-type as expected ($\Delta V_{½}$=−10.4±1.62 mV, n=4 mice, P=0.01), but basal $Rad^{-/-}$ $V_{½}$ is not significantly shifted by acute isoproterenol treatment ($\Delta V_{½}$=−1.9±0.15 mV, n=4 mice; NS), and basal $Rad^{-/-}$ $V_{½}$ is not significantly different from isoproterenol-stimulated wild-type $Rad^{-/-}$ $V_{½}$ (Figure 9A). Ca^{2+} transients fail to show increased diastolic and twitch amplitudes in RadKO cardiomyocytes in response to isoproterenol (Figure 9B through 9D). In parallel to the $I_{Ca,L}$ $V_{½}$ response, basal $Rad^{-/-}$ Ca^{2+} transients are not significantly different from those of isoproterenol-stimulated wild-type, and isoproterenol stimulation has no significant effect on $Rad^{-/-}$ (Figure 9B through 9D). Similar effects are observed from fractional sarcomere shortening (Figure 9E). Isoproterenol increases unstimulated Ca^{2+} transients in wild-type and in $Rad^{-/-}$ (Figure 9F), consistent with previous reports.[18] To further explore the protein kinase (PK)A signaling axis, we exposed cells to PKI, a cell-permeable, selective inhibitor of PKA. PKI did not reverse the elevated unstimulated Ca^{2+} transients in $Rad^{-/-}$ (Figure 9F). However, Ca^{2+} transient decay time is faster in response to isoproterenol in wild-type and $Rad^{-/-}$ (Figure 9G). Basal $Rad^{-/-}$ and wild-type decay kinetics are not significantly different (Figure 9G). Taken together, these data suggest that the effects of isoproterenol that are mediated through Rad do not affect calcium reuptake by the SR and instead shift the focus of β-adrenergic–Rad signaling primarily to the LTCC and triggering of calcium-induced calcium release.

Absence of Rad Increases Developed Pressure and Blunts β-Adrenergic Responsiveness

At the isolated cell level, sarcomeric shortening in $Rad^{-/-}$ without agonist stimulation is also indistinguishable from that of isoproterenol-stimulated wild-type cardiomyocytes (Figure 9E). This suggests functional changes at the whole heart level. $Rad^{-/-}$ mice demonstrate no difference from wild-type mice in heart weight–to–body weight ratios (Figure 10A), indicating no apparent myocardial hypertrophy. The functional data in Figure 10 demonstrate a significant increase in contractility in $Rad^{-/-}$ hearts compared with the wild-type controls. However, the contractile response to 10 nmol/L isoproterenol

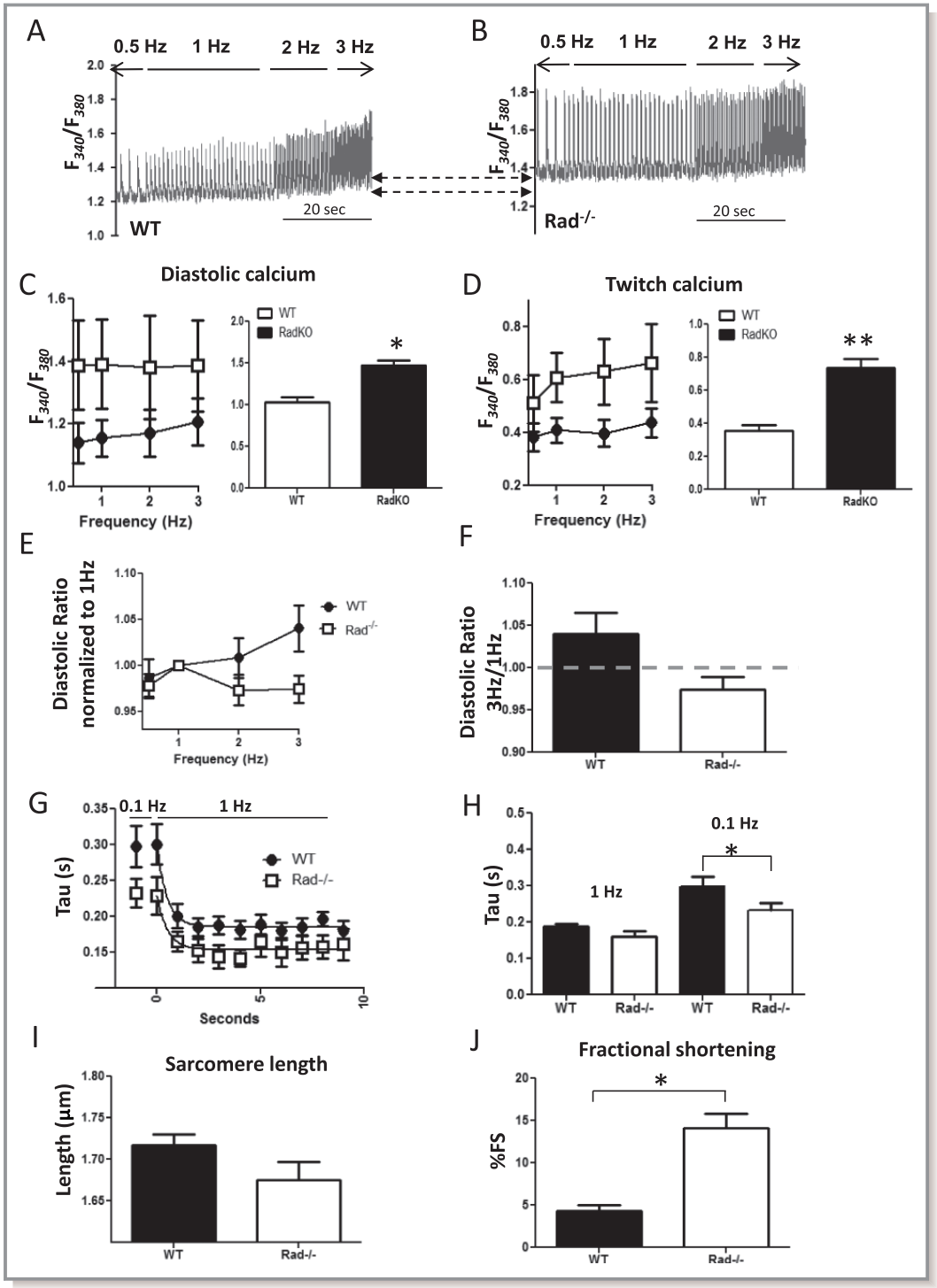

Figure 5. Diastolic calcium is elevated, dynamic range of frequency response is absent, and sarcomeric shortening is increased in Rad$^{-/-}$ cardiomyocytes. A and B, Representative $F_{340/380}$ traces in isolated adult cardiomyocytes at multiple pacing frequencies. C and D, $F_{340/380}$ ratios of wild-type (WT) and Rad$^{-/-}$ ventricular myocytes at diastole (C) and peak height (D). Bar graph: data averaged at 1 Hz. n=27 cells (5 mice) for WT, n=42 cells (8 mice) for Rad$^{-/-}$. E and F, Diastolic $F_{340/380}$ normalized to 1 Hz (E). 3 Hz to 1 Hz is shown as a measure of diastolic dynamic range (F). n=16 cells (3 mice) for WT, n=13 cells (4 mice) for Rad$^{-/-}$. G, Calcium transient decay rate (τ) of Rad$^{-/-}$ and WT as pacing is increased from 0.1 Hz to 1 Hz. n=8 cells (3 mice) for WT, n=12 cells (3 mice) for Rad$^{-/-}$. H, The change in τ is significantly different between Rad$^{-/-}$ and WT at 0.1 Hz. n=8 cells (3 mice) for WT, n=12 cells (3 mice) for Rad$^{-/-}$. I, Diastolic sarcomere length trends towards shorter in Rad$^{-/-}$. J. Fractional shortening (FS) in WT and Rad$^{-/-}$ ventricular myocytes paced at 0.1 Hz. n=16 cells (3 mice) each for WT and Rad$^{-/-}$. *P<0.05, **P<0.01, ***P<0.001 vs WT. Error bars represent SEM.

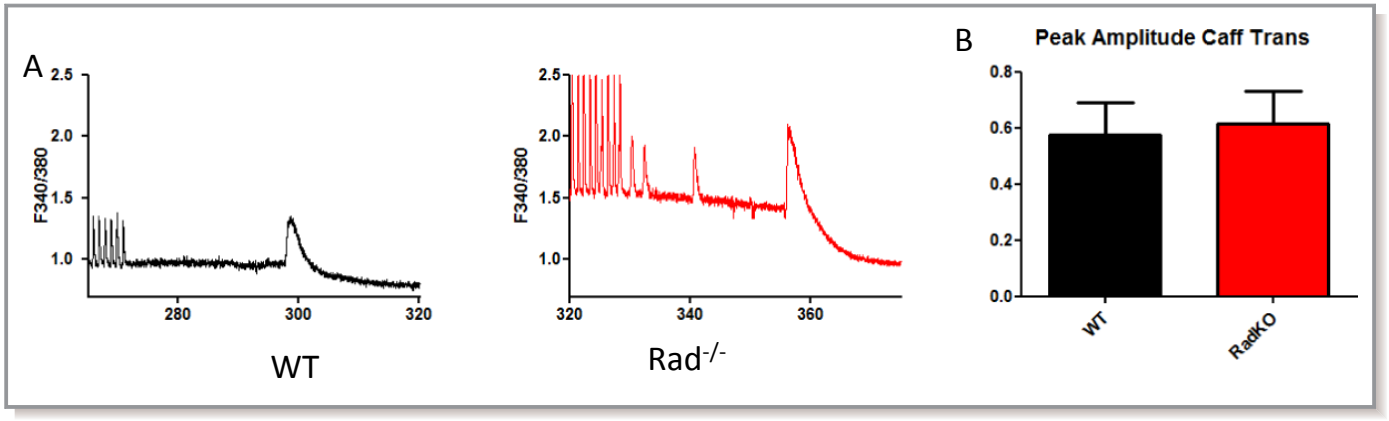

Figure 6. SR Ca^{2+} load measured as caffeine-releasable Ca^{2+} is not different between $Rad^{-/-}$ and wild-type. A, Representative traces. B, Pooled peak amplitude of caffeine induced Ca^{2+} release. SR indicates sarcoplasmic reticulum.

treatment is significantly lower in $Rad^{-/-}$ than in wild-type hearts. The relaxation velocity ($-dP/dt$) of $Rad^{-/-}$ hearts is not different from that of wild-type at baseline, but the response to isoproterenol is blunted (Figure 10B). Stroke volume data show that wild-type and $Rad^{-/-}$ hearts have a similar ejection function at baseline, whereas the response to isoproterenol treatment is blunted in $Rad^{-/-}$ hearts (Figure 10C). The effects of $Rad^{-/-}$ on cardiac function and β-adrenergic responses are also shown by the changes in systolic and diastolic left ventricular pressures compared with wild-type controls (Figure 10D). Taken together, these results are consistent with $Rad^{-/-}$ myocardium exhibiting a sympathetic agonist-like stimulated contractile state in the absence of sympathetic stimulation.

Ventricular-Triggered Arrhythmias Are Undetectable at Physiological Heart Rates

Given that diastolic Ca^{2+}-overload and sympathetic-like activity can lead to prolonged QT and cardiac rhythm disturbances, particularly ventricular ectopic beats, it is of critical importance to evaluate the impact of Rad loss on arrhythmogenesis under physiological conditions. At the level of heart function, Rad ablation increases baseline inotropic responsiveness, suggesting the possibility of Rad depletion as a new candidate therapy for increasing cardiac function. However, given that $Rad^{-/-}$ produces extraneous CaMKII-dependent unstimulated transients at subphysiological frequencies (Figure 8D and 8F), we evaluated ECGs of mice both at normal heart rate and under pharmacologically induced bradycardia to assess the risk of arrhythmia. In freely moving mice, $Rad^{-/-}$ heart rate is significantly elevated compared with wild-type (Figures 11A and 12). Acute isoproterenol treatment increases heart rate only in wild-type; no change was observed in the already elevated $Rad^{-/-}$ mice (Figure 11B), suggesting tonic sympathetic drive in $Rad^{-/-}$. Similarly, phosphorylation of phospholamban (PLB) at Ser16 is increased in hearts snap-frozen immediately after excision from $Rad^{-/-}$ mice, compared with wild-type (Figure 11C), consistent with increased sympathetic drive in $Rad^{-/-}$. Representative ECG recordings show no

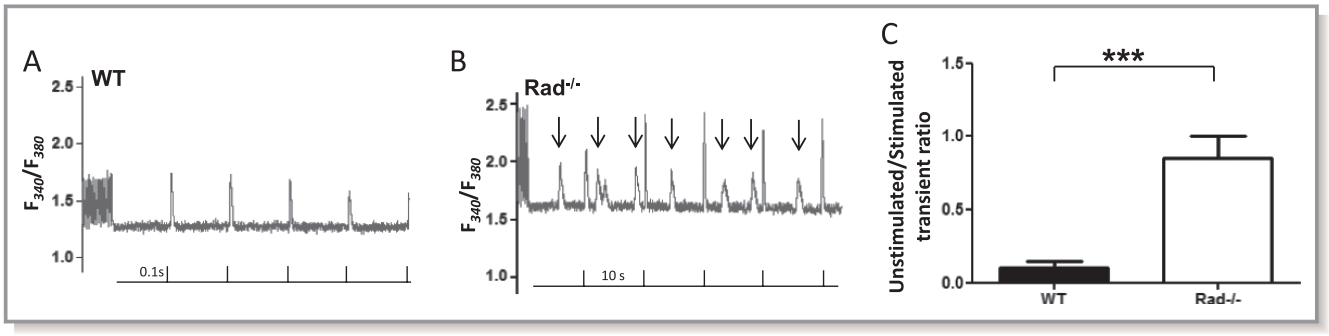

Figure 7. $Rad^{-/-}$ calcium transients display spontaneous activation at low frequency. A, Representative wild-type (WT) calcium transients showing initial 3-Hz stimulation followed by 0.1 Hz. B, Spontaneous cytosolic calcium transients spontaneously occur in isolated adult ventricular myocytes from $Rad^{-/-}$ mice paced at 0.1 Hz. Arrows indicate spontaneous transients. Solid lines with vertical tick marks indicate stimuli once every 10 s. C, Quantification of spontaneous transients in $Rad^{-/-}$ and WT cohorts. n=37 cells (5 mice) for WT, 36 cells (8 mice) for $Rad^{-/-}$. ***P<0.001 vs WT. Error bars represent SEM.

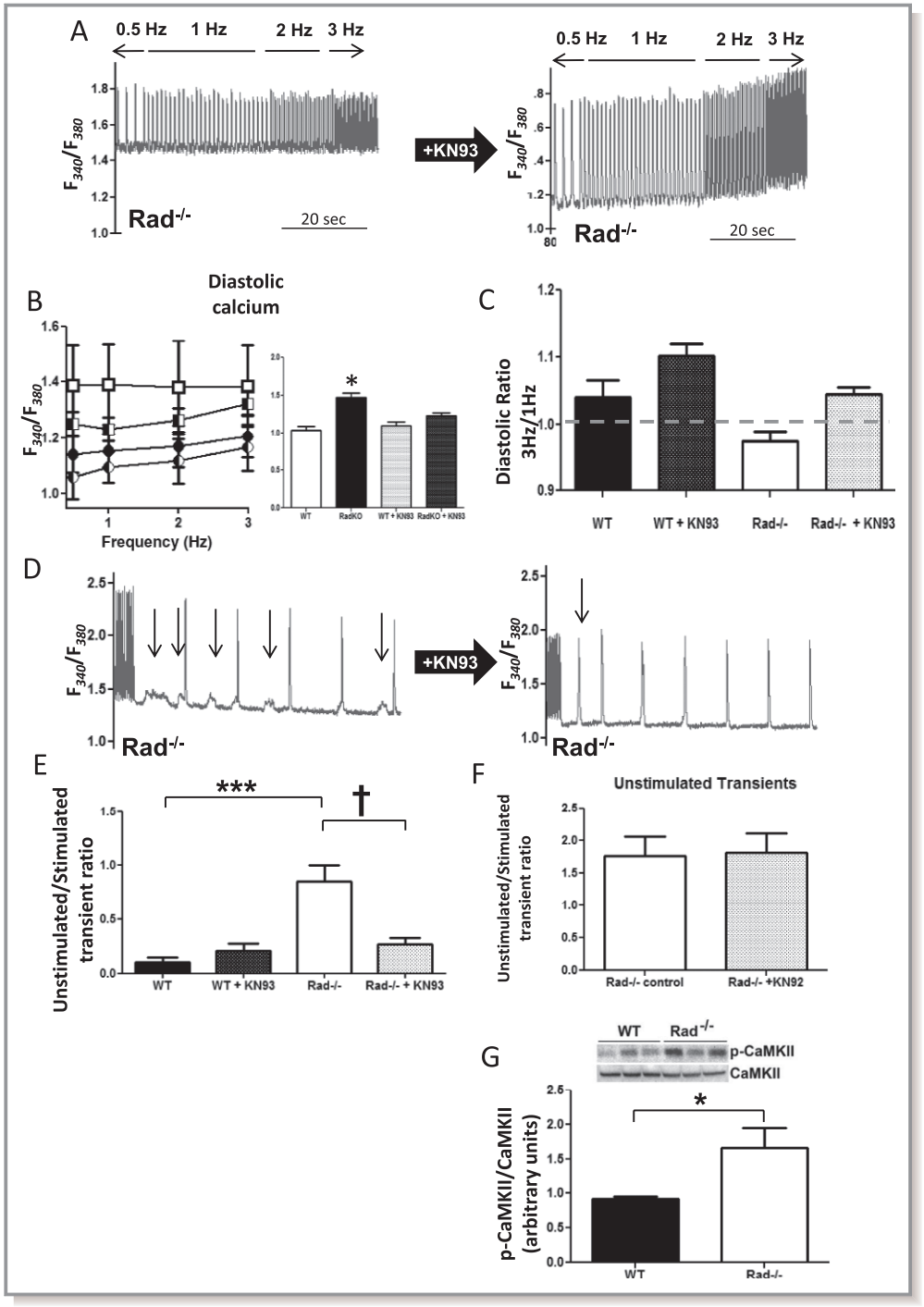

Figure 8. Elevated diastolic calcium, dynamic range response, and spontaneous transients are CaMKII dependent. A, Representative calcium transients in isolated Rad$^{-/-}$ adult cardiomyocytes at multiple pacing frequencies in the presence and absence of KN93. B, $F_{340/380}$ ratios of wild-type (WT) and Rad$^{-/-}$ ventricular myocytes at multiple frequencies at diastole. Bar graph: data averaged at 1 Hz in the presence and absence of KN93. n=27 cells (5 mice) for WT, n=42 cells (8 mice) for Rad$^{-/-}$, n=16 cells (3 mice) for WT+KN93, n=15 cells (3 mice) for Rad$^{-/-}$+KN93. C, Diastolic $F_{340/380}$ at 3 Hz normalized to 1 Hz. n=16 cells (3 mice) for WT, n=13 cells (4 mice) for Rad$^{-/-}$, n=16 cells (3 mice) for WT+KN93, n=15 cells (3 mice) for Rad$^{-/-}$+KN93. D, Representative traces of Rad$^{-/-}$ ventricular myocytes paced at 0.1 Hz in the presence and absence of KN93, demonstrating the loss of extraneous transients (arrows) when CaMKII is blocked. E, Ratio of un-stimulated transients per stimulated transient at 0.1 Hz in WT and Rad$^{-/-}$ in the presence and absence of KN93. n=37 cells (5 mice) for WT, n=36 cells (8 mice) for Rad$^{-/-}$, n=14 cells (3 mice) for WT+KN93, n=17 cells (3 mice) for Rad$^{-/-}$+KN93. F, KN-92 has no significant effect on unstimulated Ca^{2+} transients in Rad$^{-/-}$ ventricular cardiomyocytes. Unstimulated Ca^{2+} transients recorded as in Figures 4 and 5 (main text). n=12 for each group. G, CaMKII phosphorylation is greater in Rad$^{-/-}$ compared with WT. Inset above bar graph shows representative Western blots of phospho-Calmodulin kinase II (CaMKII) and CaMKII. N=7 mice for each group.*P<0.05, ***P<0.001 vs WT. †P<0.01 vs untreated. Error bars represent SEM.

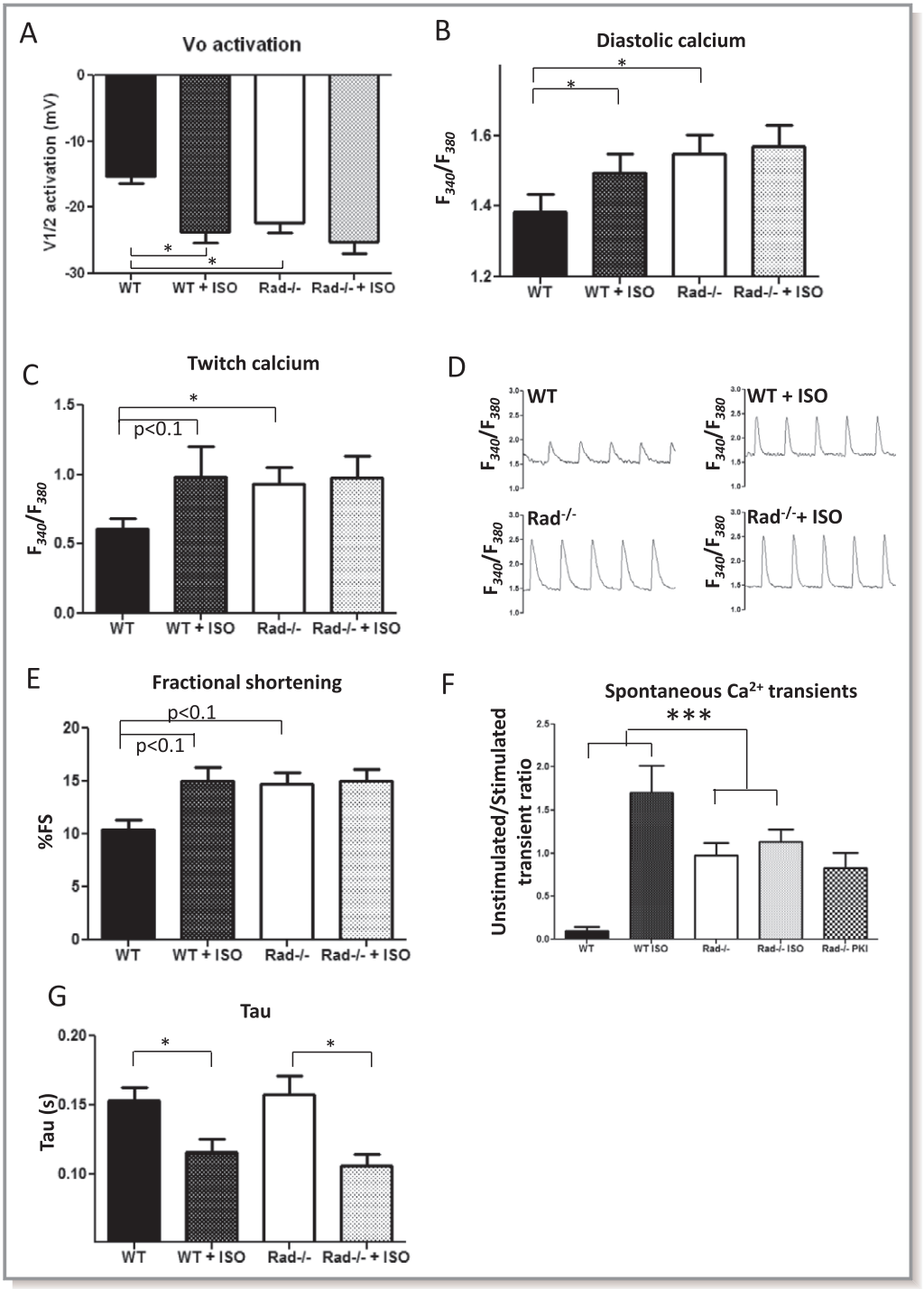

Figure 9. Basal β-adrenergic stimulation–like status and decreased response to isoproterenol (ISO) in isolated ventricular myocytes. A, $V_{½}$ activation of $I_{Ca,L}$ for wild-type (WT) (black bars) and $Rad^{-/-}$ (open bars) demonstrating a shift in WT $V_{1/2}$ but not in $Rad^{-/-}$ in response to ISO. B through E, Calcium cycling parameters and representative traces in $Rad^{-/-}$ cells demonstrate no response to ISO stimulation. Diastolic calcium ratio (B), transient peak amplitude (C), Representative Ca^{2+} transients for WT and $Rad^{-/-}$ before and after acute ISO addition (D), and fractional shortening (FS) (E) were significantly higher in $Rad^{-/-}$ compared with WT in untreated hearts, and remained unchanged in the presence of ISO in $Rad^{-/-}$. n=12 cells (3 mice) for WT, n=18 cells (3 mice) for $Rad^{-/-}$. F, Spontaneous Ca^{2+} transients in WT are increased by ISO, but $Rad^{-/-}$ show no significant response. N=μmol/L PKI had no effect on $Rad^{-/-}$ spontaneous Ca^{2+} transients. n=37 cells (5 mice) for WT, n=36 cells (8 mice) for $Rad^{-/-}$, n=11 cells (3 mice) for WT+ISO, n=16 cells (3 mice) for $Rad^{-/-}$+ISO. G, In $Rad^{-/-}$ cells, tau (τ), a measure of calcium re-uptake kinetics, responded significantly to ISO, similar to WT cohorts n=12 cells (3 mice) for WT, n=18 cells (3 mice) for $Rad^{-/-}$. **P*<0.05, ***P*<0.01,****P*<0.001 vs WT. Error bars represent SEM. NS indicates not significant, $V_{½}$, activation midpoint; $I_{Ca,L}$, L-type calcium channel; PKI, protein kinase I.

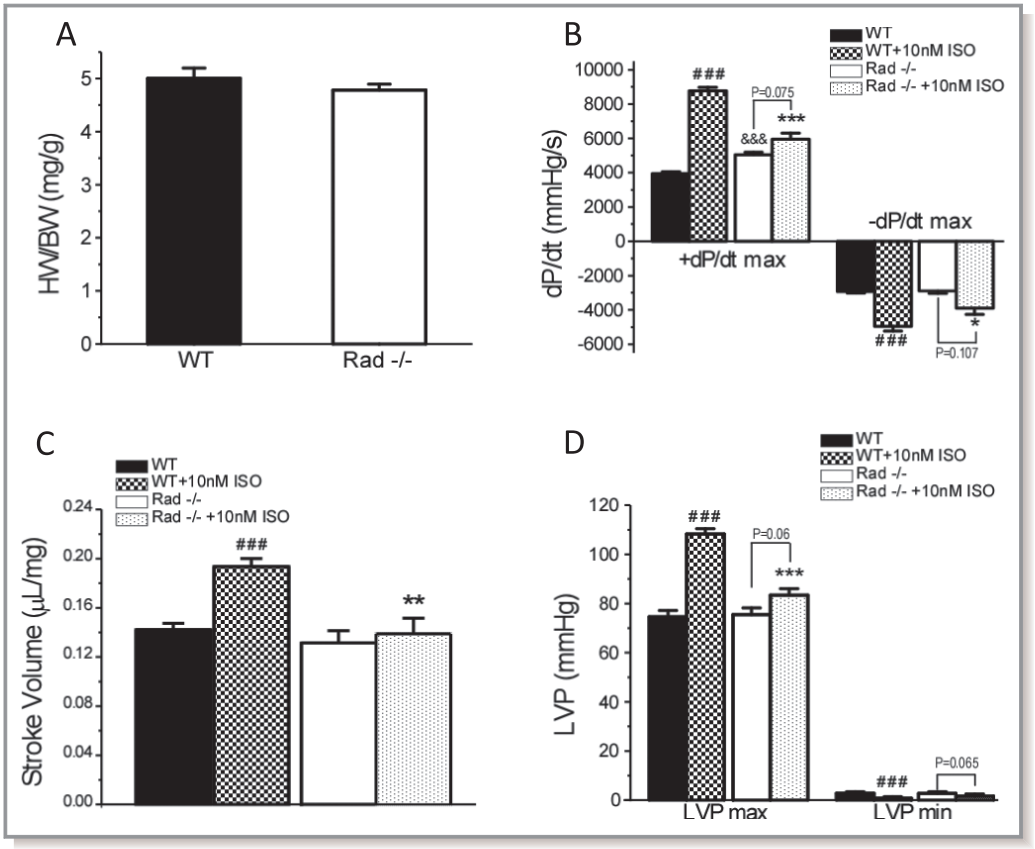

Figure 10. Baseline and β-adrenergic stimulated function of ex vivo Rad$^{-/-}$ and wild-type (WT) working hearts. A, Rad$^{-/-}$ and WT mice demonstrated no difference in heart weight (HW)–to–body weight (BW) ratios. n=5 WT mice, 5 Rad$^{-/-}$ mice. B, A significant increase in contractility (contractile velocity, +dP/dt) was observed in Rad$^{-/-}$ hearts compared with WT, while the contractile response to isoproterenol (ISO) treatment was significantly lower than WT. The relaxation velocity (−dP/dt) of Rad$^{-/-}$ was not different from WT at baseline but the response to ISO was blunted. n=5 WT mice, 5 Rad$^{-/-}$ mice. C, Stroke volume measurements showed that Rad$^{-/-}$ hearts had similar ejecting function to that of WT at baseline, whereas the response to ISO treatment was blunted n=5 WT mice, 5 Rad$^{-/-}$ mice. D, The effects of Rad$^{-/-}$ on cardiac function and β-adrenergic responses were further shown by the changes in systolic and diastolic left ventricular pressures (LVP) compared with WT controls. n=5 WT mice, 5 Rad$^{-/-}$ mice. &&&, P<0.001 vs WT control in Student t test; ###, P<0.001 vs WT control in paired Student t test; *P<0.05, **P<0.01, ***P<0.001 vs WT under ISO treatment in Student t test. Error bars represent SEM.

apparent differences between wild-type and Rad$^{-/-}$ under baseline conditions (Figure 11D). No ventricular arrhythmias were observed in either group of mice. We postulated that the relatively high heart rate of the Rad$^{-/-}$ mouse, a form of overdrive suppression, protects the heart against Ca^{2+} overload, presumably secondary to accumulated inactivation of LTCC. Building on cellular findings that relatively low stimulation frequencies unmask afterdepolarizations and spontaneous Ca^{2+} transients, we then challenged mice with acute muscarinic agonist (carbachol) to dramatically lower heart rate (Figure 11E). Using the method of Mitchell and colleagues,[19] we plotted QT as a function of RR interval and lnQT as a function of lnRR(100), where RR is normalized to average RR (100 ms) (Figure 11F). Carbachol prolongs both RR and QT intervals in a linear relationship as expected, although in Rad$^{-/-}$, QT elongation becomes more pronounced at lower frequencies (Figure 11F). At baseline, the rate-corrected QT interval (QTc) is not significantly different between wild-type and Rad$^{-/-}$ (Figure 11G). Similarly, QTc in Rad$^{-/-}$ mice is significantly elevated by carbachol-prolonged RR intervals (Figure 11H), compared with wild-type, resulting in a significant sharp increase in the estimated slope of the relationship between lnQT and lnRR(100) (Figure 11F). Therefore, only at extreme subphysiological heart rates does Rad ablation show QT prolongation. It should be noted that we did not observe this to be accompanied by increases in ventricular arrhythmia incidence (data not shown).

Discussion

This study is the first to show that the absence of Rad expression in the heart results in significantly increased contractile function commensurate with elevated Ca^{2+} entry at relatively negative membrane potentials and increased developed pressure without detectable arrhythmias or cellular Ca^{2+} overload at physiological heart rates. Slow heart rate (or

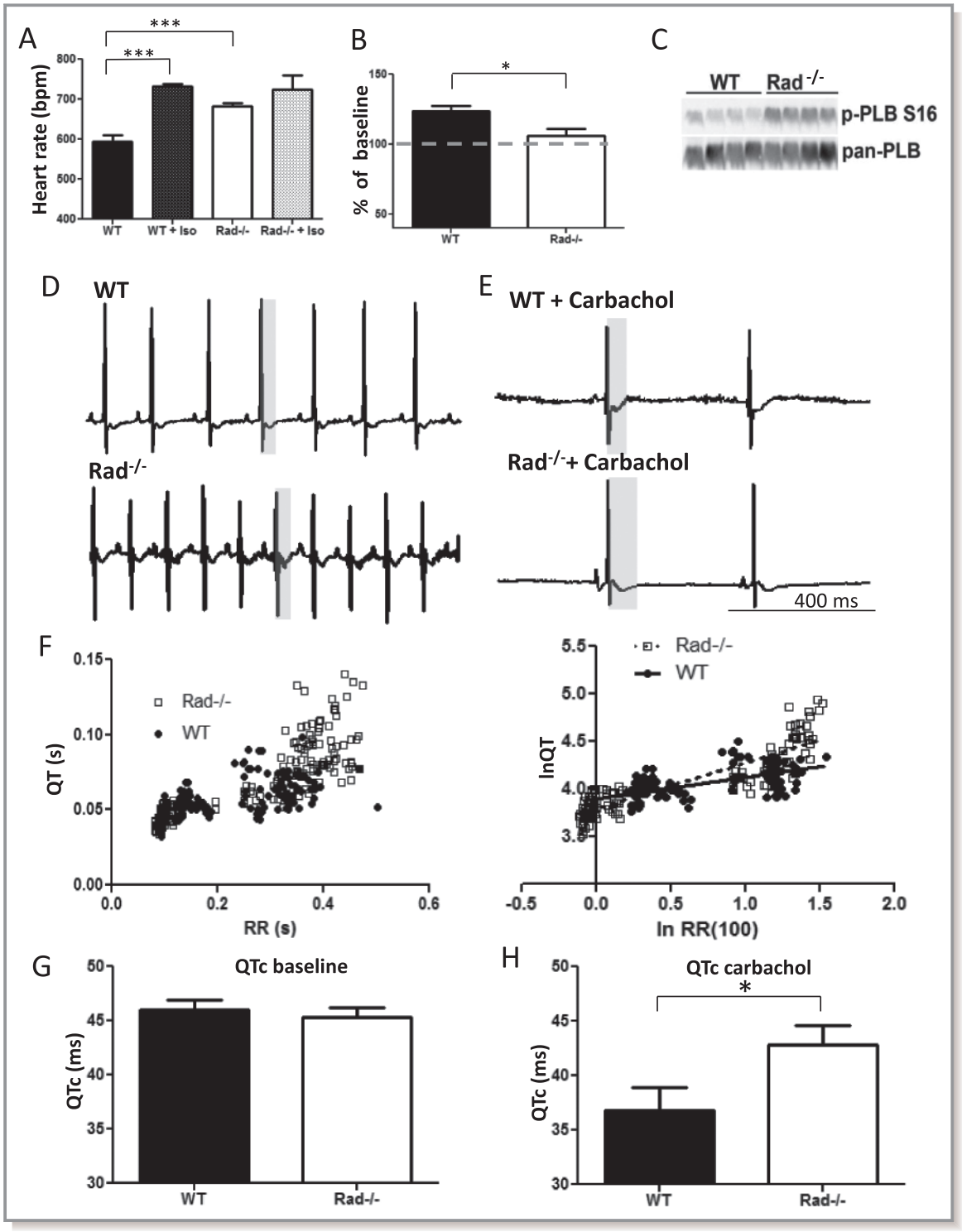

Figure 11. Heart rate and QT intervals are altered in intact Rad$^{-/-}$ mice. A, Average heart rate for Rad$^{-/-}$ mice is elevated compared with wild-type (WT) cohorts. n=10 WT mice, n=13 Rad$^{-/-}$ mice. B, Heart rates in Rad$^{-/-}$ mice display a reduced response to isoproterenol, indicating a sympathetically driven phenotype. n=6 WT mice, n=6 Rad$^{-/-}$ mice. C, Immunoblots demonstrating that phospholamban phosphorylation at residue serine 16 is elevated in Rad$^{-/-}$ hearts relative to WT hearts. D and E, Representative ECGs of WT and Rad$^{-/-}$ before and after carbachol-induced bradycardia. Highlighted region indicates QT segment. F, Plotting QT against RR intervals and lnQT intervals against lnRR(100) reveals an altered linear relationship at high RR intervals (low frequency) in Rad$^{-/-}$ mice, suggesting a frequency dependent QT elongation n=10 WT mice, n=13 Rad$^{-/-}$ mice. G, Corrected QT (QTc) segments are not significantly different between untreated WT and Rad$^{-/-}$. n=10 WT mice, n=13 Rad$^{-/-}$ mice. H, QTc segments in Rad$^{-/-}$ mice are significantly higher than WT segments after carbachol treatment. n=10 WT mice, n=13 Rad$^{-/-}$ mice. *P<0.05, ***P<0.001 vs WT. Error bars represent SEM.

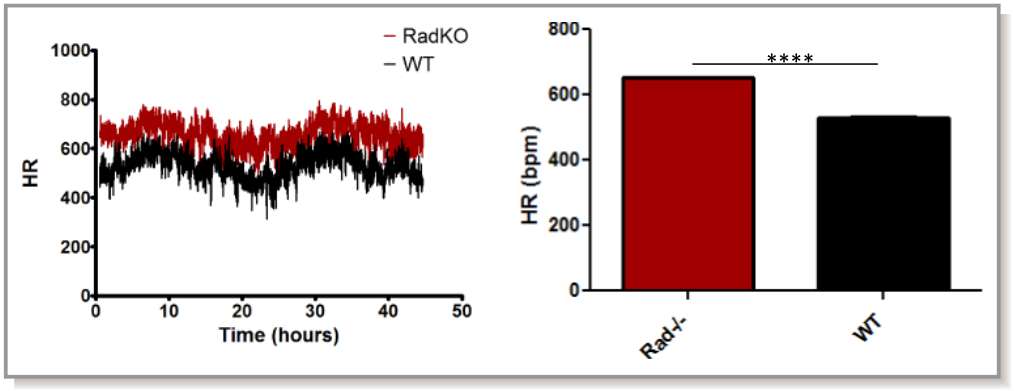

Figure 12. Faster heart rate in Rad$^{-/-}$ compared with wild-type (WT) mice. Heart rate was captured. Left, Representative 48-hour continuous recording from a Rad$^{-/-}$ and WT mouse. Circadian rhythm of heart rate is present in both (mice on 12-hour light/12-hour dark cycle), and Rad$^{-/-}$ heart rate is faster for all times of day. Right, Pooled data of mean 24-hour heart rate. n=6 Rad$^{-/-}$ mice; n=7 wt mice, ****$P<10^{-4}$ vs WT.

slow stimulation frequency) coupled with an increased $I_{Ca,L}$ window current in Rad$^{-/-}$ cardiomyocytes leads to spontaneous Ca^{2+} transients and afterdepolarizations at the cellular level, but only for ultraslow, nonphysiological frequencies. Our new results suggest that β-adrenergic modulation of contractile Ca^{2+} requires the presence of Rad. Under basal conditions, Rad$^{-/-}$ electrical and contractile properties were not significantly different from that in wild-type cells and hearts under β-adrenergic stimulation. In Rad$^{-/-}$ mice $I_{Ca,L}$, Ca^{2+} transients, and cell shortening exhibited β-adrenergic receptor stimulation-like properties, despite the absence of β-receptor agonist. This cellular finding underpins the significantly enhanced contractility of intact Rad$^{-/-}$ hearts. Taken together, these results are consistent with the new provocative hypothesis that β-adrenergic signaling of contractile Ca^{2+} functions in part via disinhibition of Rad-$I_{Ca,L}$ function.

Relationship to Previous Studies of Rad in the Heart

The present work is the first to evaluate the electrophysiological and contractile mechanisms responsible for Rad-deletion–induced alterations in myocardial function. Our work builds on results from 3 previous studies exploring Rad contributions to cardiomyocyte function. Two studies used overexpression of Rad or Rad mutants.[13,20] Overexpression of a dominant negative form of Rad showed a hyperpolarized shift of the LTCC activation curve consistent with our results.[21] Only one study known to us considers Rad$^{-/-}$ mice,[14] which examines hypertrophic growth but leaves open the question of the role of calcium on electrical and contractile parameters. This study showed no gross changes in the morphology of the heart at baseline,[14] consistent with the present study (Figure 10A). Rad$^{-/-}$ mice were more susceptible to pressure overload hypertrophy commensurate with increased activity of CaMKII.[14] Increased diastolic and window $I_{Ca,L}$ promote elevated CaMKII and thus provide a logical mechanism to explain the priming of increased autophosphorylated CaMKII in our study (Figure 8). We now show increased window $I_{Ca,L}$ in the Rad$^{-/-}$ cardiomyocyte (Figure 1). Thus, it is plausible that any event that promotes depolarization will increase calcium influx. In turn, increased calcium influx can promote CaMKII activation.

Hypertrophy Fails to Develop Despite Sustained Elevated Calcium Levels

It is intriguing that loss of Rad did not produce a hypertrophic phenotype in unchallenged hearts[14] (Figure 10A). It is somewhat surprising that a sustained increase in calcium influx and intracellular calcium levels do not trigger cell hypertrophic cardiomyocyte growth, although it is worth noting that pressure-induced hypertrophy is more severe in Rad$^{-/-}$ mice.[14] A solution to this paradox may lie in functional differences between calcium-handling proteins in different subcellular domains. For example, LTCCs targeted to microdomains enriched with caveolin-3 regulate calcium-mediated growth signaling independent of contraction and beat-to-beat calcium homeostasis.[21,22] Given the results presented here, we predict that Rad plays a role in the regulation of channels that modulate twitch calcium but does not alter calcium-induced growth signaling pathways under normal physiological circumstances. Determining whether Rad localizes to restricted membrane domains in concert with LTCC compartmentalization[23] is an important future direction.

Rad Electrical Mechanisms of Action

This is the first study to evaluate the electrophysiological effects of Rad deletion in the heart. Given that the overexpression of Rad has been shown to produce block of I_{CaL}, it is unsurprising that Rad deletion increases LTCC current.[9]

Previous studies have determined that Rad directly binds primarily to the β subunit of $Ca_V1.2$[9] and, interestingly, the activation curve of $Rad^{-/-}$ resembles models of increased $Ca_V\beta2a$ expression, where the voltage dependence of the activated current is shifted to hyperpolarizing and channels open at less-depolarized potentials, resulting in increased calcium current.[24,25] The present study is also the first to examine the effect of prolonging the stimulation frequency on $Rad^{-/-}$ mice at both the cellular and whole animal levels, suggesting for the first time that lowering the heart rate far below physiological rates produces an arrhythmogenic trigger.

We also demonstrate here that Rad deletion results in an apparent loss of β-AR responsiveness, and this is consistent with the new hypothesis that Rad deletion causes LTCC functional modifications that mimic tonic β-AR–like stimulation with respect to trigger Ca^{2+}. This includes a leftward shift of the I_{CaL} activation curve, changes to both systolic and diastolic calcium levels, increased contractility, and increased transient decay rates at low pacing frequency. This result mirrors the findings of Wang and colleagues,[13] who demonstrate that overexpression of Rad blocks calcium current in both control and isoproterenol-stimulated heart cells. However, they also demonstrated that Rad knockdown to 30% of normal expression did not alter the results of β-AR stimulation, which contrasts with our findings that complete Rad deletion has profound effects on the contractile signaling downstream of β-AR activation. Taken together, these data suggest that 30% of Rad expression may be sufficient to retain acute effects of isoproterenol. We suggest that the mechanism of this action in wild-type myocardium is that Rad normally acts as a tonic block on I_{CaL}, which is then removed upon β-AR stimulation. In parallel, α-adrenergic stimulation has been shown in vitro to lead to RGK protein phosphorylation, which in turn relieves $Ca_V1.2$ inhibition.[26] $Rad^{-/-}$ constitutive gain of function with respect to β-AR phenotype should also be weighed in context of $Ca_V\beta$-subunit contribution to PKA signaling. Overexpression of $Ca_V\beta2$ isoforms follows a saturable function, suggesting an unidentified limiting resource in PKA-$I_{Ca,L}$ signaling.[27] Our present data are consistent with the speculative new hypothesis that Rad-channel occupancy represents such a limiting resource as postulated by Colecraft and colleagues.[27] In the absence of Rad, the dynamic range for PKA signaling may be reduced because activation of the channel complex is in a tonic ON state.

$I_{Ca,L}$ decay kinetics in cardiomyocytes are dominated by calcium-dependent inactivation.[28,29] In sodium-free bath conditions, the early component of $I_{Ca,L}$ decay is related to SR Ca^{2+} release.[30–32] It therefore follows that increased Ca^{2+} release in $Rad^{-/-}$ can drive apparent faster decay kinetics (Figure 1C). We can speculate that this would represent an inherent negative feedback pathway to blunt the increased macroscopic conductance and shifted activation curve in $Rad^{-/-}$ cardiomyocytes. The finding that a relatively fast decay persists at potentials as negative as −30 mV corresponds with the increased LTCC opening at such low voltages.

Ca^{2+} transient decay kinetics are determined by the interplay of regulators of Ca^{2+} homeostasis. In the mouse, the SR provides the vast majority of contractile Ca^{2+}, and therefore a major determinant of Ca^{2+} transient kinetics is the activity of SR reuptake by the sarcoendoplasmic reticulum calcium transport ATPase (SERCa)-PLB complex. However, FDAR, first described by Bowditch in 1871, is not dependent on PLB,[33] but is modified by CaMKII.[34] The blunting of FDAR in $Rad^{-/-}$ (Figure 5G and 5H) is consistent with the notion that LTCC-Rad CaMKII signaling axis contributes to FDAR.

Significance

Rad levels are significantly decreased in failing human hearts[14] consistent with the idea supported by our study that Rad depletion provides a compensatory positive inotropic response. The identification of Rad as an integral regulator of β-AR–mediated increases in calcium channel influx produces a potential therapeutic target in widespread patient populations requiring inotropic support. Our results suggest that Rad depletion preferentially targets LTCC trigger Ca^{2+}, bypassing the β-AR signaling axis to increase the inotropic response.

Acknowledgments

We are grateful to Dr C. Ronald Kahn, Joslin Diabetes Center, Harvard Medical School, for the $Rad^{-/-}$ mice. We are grateful to Tanya Seward and Karyn Esser for radiotelemetry support from the UK Center of Muscle Biology and to Brian Delisle for insightful discussions and critical review of this work.

Sources of Funding

This work was supported by National Institutes of Health grants HL072936 (D.A.A. and J.S.), HL074091 (J.S.), and HL098945 (J.P.J.), by grant 2P20 RR020171 from the National Center for Research Resources (D.A.A.), and by University of Kentucky 2012–2013 Research Professorship (D.A.A.). C.N.K. was supported by T32-HL072743.

Disclosures

None.

References

1. Yancy CW, Jessup M, Bozkurt B, Butler J, Casey DE Jr, Drazner MH, Fonarow GC, Geraci SA, Horwich T, Januzzi JL, Johnson MR, Kasper EK, Levy WC, Masoudi FA, McBride PE, McMurray JJ, Mitchell JE, Peterson PN, Riegel B, Sam F, Stevenson LW, Tang WH, Tsai EJ, Wilkoff BL. 2013. ACCF/AHA guideline for the management of heart failure: a report of the American College of

Cardiology Foundation/American Heart Association Task Force on Practice Guidelines. *Circulation*. 2013;128:1810–1852.

2. Bers DM. Calcium cycling and signaling in cardiac myocytes. *Annu Rev Physiol*. 2008;70:23–49.
3. Qi X, Yeh YH, Chartier D, Xiao L, Tsuji Y, Brundel BJ, Kodama I, Nattel S. The calcium/calmodulin/kinase system and arrhythmogenic afterdepolarizations in bradycardia-related acquired long-QT syndrome. *Circ Arrhythm Electrophysiol*. 2009;2:295–304.
4. Wu Y, MacMillan LB, McNeill RB, Colbran RJ, Anderson ME. CaM kinase augments cardiac L-type Ca^{2+} current: a cellular mechanism for long Q-T arrhythmias. *Am J Physiol*. 1999;276:H2168–H2178.
5. Weiss JN, Nivala M, Garfinkel A, Qu Z. Alternans and arrhythmias: from cell to heart. *Circ Res*. 2011;108:98–112.
6. Riccio ML, Koller ML, Gilmour RF Jr. Electrical restitution and spatiotemporal organization during ventricular fibrillation. *Circ Res*. 1999;84:955–963.
7. Mahajan A, Sato D, Shiferaw Y, Baher A, Xie LH, Peralta R, Olcese R, Garfinkel A, Qu Z, Weiss JN. Modifying L-type calcium current kinetics: consequences for cardiac excitation and arrhythmia dynamics. *Biophys J*. 2008;94:411–423.
8. Flynn R, Zamponi GW. Regulation of calcium channels by RGK proteins. *Channels (Austin)*. 2010;4:434–439.
9. Finlin BS, Crump SM, Satin J, Andres DA. Regulation of voltage-gated calcium channel activity by the Rem and Rad GTPases. *Proc Natl Acad Sci USA*. 2003;100:14469–14474.
10. Beguin P, Ng YJ, Krause C, Mahalakshmi RN, Ng MY, Hunziker W. RGK small GTP-binding proteins interact with the nucleotide kinase domain of Ca^{2+}-channel beta-subunits via an uncommon effector binding domain. *J Biol Chem*. 2007;282:11509–11520.
11. Finlin BS, Correll RN, Pang C, Crump SM, Satin J, Andres DA. Analysis of the complex between Ca^{2+} channel beta-subunit and the Rem GTPase. *J Biol Chem*. 2006;281:23557–23566.
12. Magyar J, Kiper CE, Sievert G, Cai W, Shi GX, Crump SM, Li L, Niederer SA, Smith NP, Andres DA, Satin J. Rem-GTPase regulates cardiac myocyte L-type calcium current. *Channels (Austin)*. 2012;6:1–8.
13. Wang G, Zhu X, Xie W, Han P, Li K, Sun Z, Wang Y, Chen C, Song R, Cao C, Zhang J, Wu C, Liu J, Cheng H. Rad as a novel regulator of excitation-contraction coupling and beta-adrenergic signaling in heart. *Circ Res*. 2010;106:317–327.
14. Chang L, Zhang J, Tseng YH, Xie CQ, Ilany J, Bruning JC, Sun Z, Zhu X, Cui T, Youker KA, Yang Q, Day SM, Kahn CR, Chen YE. Rad GTPase deficiency leads to cardiac hypertrophy. *Circulation*. 2007;116:2976–2983.
15. Tomaselli GF, Zipes DP. What causes sudden death in heart failure? *Circ Res*. 2004;95:754–763.
16. Feng HZ, Biesiadecki BJ, Yu ZB, Hossain MM, Jin JP. Restricted N-terminal truncation of cardiac troponin T: a novel mechanism for functional adaptation to energetic crisis. *J Physiol*. 2008;586:3537–3550.
17. Pang C, Crump SM, Jin L, Correll RN, Finlin BS, Satin J, Andres DA. Rem GTPase interacts with the proximal CaV1.2 C-terminus and modulates calcium-dependent channel inactivation. *Channels (Austin)*. 2010;4:192–202.
18. Curran J, Hinton MJ, Rios E, Bers DM, Shannon TR. Beta-adrenergic enhancement of sarcoplasmic reticulum calcium leak in cardiac myocytes is mediated by calcium/calmodulin-dependent protein kinase. *Circ Res*. 2007;100:391–398.
19. Mitchell GF, Jeron A, Koren G. Measurement of heart rate and Q-T interval in the conscious mouse. *Am J Physiol*. 1998;274:H747–H751.
20. Yada H, Murata M, Shimoda K, Yuasa S, Kawaguchi H, Ieda M, Adachi T, Murata M, Ogawa S, Fukuda K. Dominant negative suppression of Rad leads to QT prolongation and causes ventricular arrhythmias via modulation of L-type Ca^{2+} channels in the heart. *Circ Res*. 2007;101:69–77.
21. Makarewich CA, Correll RN, Gao H, Zhang H, Yang B, Berretta RM, Rizzo V, Molkentin JD, Houser SR. A caveolae-targeted L-type Ca(2)+ channel antagonist inhibits hypertrophic signaling without reducing cardiac contractility. *Circ Res*. 2012;110:669–674.
22. Foell JD, Balijepalli RC, Delisle BP, Yunker AM, Robia SL, Walker JW, McEnery MW, January CT, Kamp TJ. Molecular heterogeneity of calcium channel beta-subunits in canine and human heart: evidence for differential subcellular localization. *Physiol Genomics*. 2004;17:183–200.
23. Balijepalli RC, Foell JD, Hall DD, Hell JW, Kamp TJ. Localization of cardiac L-type Ca(2+) channels to a caveolar macromolecular signaling complex is required for beta(2)-adrenergic regulation. *Proc Natl Acad Sci USA*. 2006;103:7500–7505.
24. Colecraft HM, Alseikhan B, Takahashi SX, Chaudhuri D, Mittman S, Yegnasubramanian V, Alvania RS, Johns DC, Marban E, Yue DT. Novel functional properties of Ca(2+) channel beta subunits revealed by their expression in adult rat heart cells. *J Physiol*. 2002;541:435–452.
25. Chen X, Nakayama H, Zhang X, Ai X, Harris DM, Tang M, Zhang H, Szeto C, Stockbower K, Berretta RM, Eckhart AD, Koch WJ, Molkentin JD, Houser SR. Calcium influx through CaV1.2 is a proximal signal for pathological cardiomyocyte hypertrophy. *J Mol Cell Cardiol*. 2011;50:460–470.
26. Jhun BS, O-Uchi J, Wang W, Ha CH, Zhao J, Kim JY, Wong C, Dirksen RT, Lopes CM, Jin ZG. Adrenergic signaling controls RGK-dependent trafficking of cardiac voltage-gated L-type Ca^{2+} channels through PKD1. *Circ Res*. 2012;110:59–70.
27. Miriyala J, Nguyen T, Yue DT, Colecraft HM. Role of CaVbeta subunits, and lack of functional reserve, in protein kinase A modulation of cardiac CaV1.2 channels. *Circ Res*. 2008;102:e54–e64.
28. Grandi E, Morotti S, Ginsburg KS, Severi S, Bers DM. Interplay of voltage and Ca-dependent inactivation of L-type Ca current. *Prog Biophys Mol Biol*. 2010;103:44–50.
29. Alseikhan BA, DeMaria CD, Colecraft HM, Yue DT. Engineered calmodulins reveal the unexpected eminence of Ca^{2+} channel inactivation in controlling heart excitation. *Proc Natl Acad Sci USA*. 2002;99:17185–17190.
30. Bourgonje VJ, Vos MA, Ozdemir S, Doisne N, Acsai K, Varro A, Sztojkov-Ivanov A, Zupko I, Rauch E, Kattner L, Bito V, Houtman M, van der Nagel R, Beekman JD, van Veen TA, Sipido KR, Antoons G. Combined Na+/Ca^{2+} exchanger and L-type calcium channel block as a potential strategy to suppress arrhythmias and maintain ventricular function. *Circ Arrhythm Electrophysiol*. 2013;6:371–379.
31. Bito V, Heinzel FR, Biesmans L, Antoons G, Sipido KR. Crosstalk between L-type Ca^{2+} channels and the sarcoplasmic reticulum: alterations during cardiac remodelling. *Cardiovasc Res*. 2008;77:315–324.
32. Pott C, Yip M, Goldhaber JI, Philipson KD. Regulation of cardiac L-type Ca^{2+} current in Na+-Ca^{2+} exchanger knockout mice: functional coupling of the Ca^{2+} channel and the Na+-Ca^{2+} exchanger. *Biophys J*. 2007;92:1431–1437.
33. DeSantiago J, Maier LS, Bers DM. Frequency-dependent acceleration of relaxation in the heart depends on CaMKII, but not phospholamban. *J Mol Cell Cardiol*. 2002;34:975–984.
34. Picht E, DeSantiago J, Huke S, Kaetzel MA, Dedman JR, Bers DM. CaMKII inhibition targeted to the sarcoplasmic reticulum inhibits frequency-dependent acceleration of relaxation and Ca^{2+} current facilitation. *J Mol Cell Cardiol*. 2007;42:196–205.